High-harmonic generation in interfering waves

A. V. Birulin, V. T. Platonenko, and V. V. Strelkov

M. V. *Lomonosov State University, 119899 Moscow, Russia*

A theoretical model is developed for the description of high-harmonic generation in a field of two waves interfering in a homogeneous or inhomogeneous dispersive medium (in a gas or rarefied plasma layer). It is shown that the use of two crossing or counterpropagating beams in high-harmonic generation experiments provides a means for canceling or partially canceling dispersion, significantly enhancing the generation efficiency, and producing harmonics that emanate from the layer at different angles. © *1996 American Institute of Physics.*
[S1063-7761(96)00607-5]

1. INTRODUCTION

The high-harmonic generation observed when atoms or ions in gas jets[1–4] or in a rarefied plasma[5,6] are exposed to intense light is one of the most interesting objects of investigation in modern laser physics. It takes place in light beams with intensities of 10^{13} W/cm^2 or higher, depending on the properties of the atomic particles. For stimulating radiation of sufficiently high intensity, a broad plateau containing dozens of odd harmonics and having a relatively sharp high-frequency cutoff is observed in the harmonic spectrum.

High-harmonic generation can be interpreted roughly as the periodically repeated tunneling ionization of particles and subsequent radiative recombination of its products. The periodicity of the process imparts a discrete structure to the spectrum. It follows from symmetry considerations that the spectrum must contain only odd harmonics (provided that the stimulating radiation is smoothly activated). The width of the spectrum can be estimated from the conservation of energy. The low-frequency limit of the plateau must be close to the ionization energy of the atom. (Actually it is usually shifted toward the low-frequency end.) According to theoretical studies,[7,8] the high-frequency limit must lie in the range of quantum energies close to $\hbar\omega = I + 3U$, where I is the ionization potential, and U is the ponderomotive electron energy. The uncertainty of the intensity at which generation actually takes place makes it difficult to verify this relation experimentally, but experiments show, on the whole, that the energy of harmonics obtainable from certain atoms is higher, the more stable those atoms are against ionization. The very shortest wavelengths obtained to date lie in the vicinity of 6 nm (Ref. 4). It seems likely that further advancement down the wavelength scale should be possible by using ions, which have higher ionization potentials and greater stability in the presence of a field than atoms. Experiments on the generation of high harmonics in a plasma are reported, for example, in Refs. 5 and 6.

In principle, high-harmonic generation can emerge as an important practical method for the production of coherent x-rays. As a rule, unfortunately, the efficiency of this process is very low. Most studies published so far have addressed the generation of harmonics of the highest possible order and frequencies. The problem of optimizing the efficiency is

mentioned, for example, in Ref. 3, where the choice of experimental conditions was such as to achieve an efficiency of 10^{-6} in the conversion (in xenon) of neodymium laser radiation into the 17th harmonic. The efficiency measured in the same paper for conversion to harmonics with wavelengths in the vicinity of 8 nm was approximately 10^{-9} (in neon).

One cause of the low efficiency is dispersion of the working media, which limits the number of particles in the layer where generation can be assisted by mode locking. In principle, mode-locking conditions can be established by utilizing resonances of the medium and a special choice of frequency of the stimulating radiation.[9] The exploitation of this possibility appears to be limited to the range of intensities at which resonance transitions are still weakly excited. In the case of media whose refractive index exhibits a monotonic or almost-monotonic frequency dependence (e.g., plasma) it is virtually impossible to satisfy the mode-locking conditions in experiments on high-harmonic generation in a conventional single-beam geometry.

In this study we discuss the feasibility of satisfying the mode-locking conditions for high-harmonic generation in crossing or counterpropagating beams. In this kind of geometry, processes other than the usual

$$n(\omega,\mathbf{k}) \to (n\omega, \mathbf{k}(n\omega)), \tag{1.1}$$

where $(\omega, \mathbf{k})$ denotes a quantum of energy $\hbar\omega$ and momentum $\hbar\mathbf{k}$, and n is an integer, are also possible; for example,

$$(n \pm j)(\omega, \mathbf{k}_1) \mp j(\omega, \mathbf{k}_2) \to (n\omega, \mathbf{k}(n\omega)). \tag{1.2}$$

If the frequency $n\omega$ is situated in the plateau region and if the number j is not too high, the elementary processes (1.1) and (1.2) can have comparable efficiencies. On the other hand, the mode-locking condition in processes (1.2) can be guaranteed, for example, by the proper choice of density of the medium or angles between $\mathbf{k}_1$ and $\mathbf{k}_2$, even if the refractive index of the medium varies monotonically with the frequency.

In principle, the setup of experiments on high-harmonic generation in "colliding" beams (Fig. 1) can lead to significant enhancement of the generation efficiency. It can also provide new information about the physics of the phenomenon. Consequently, a preliminary theoretical analysis of the efficiency of such generation is very timely. The main objec-
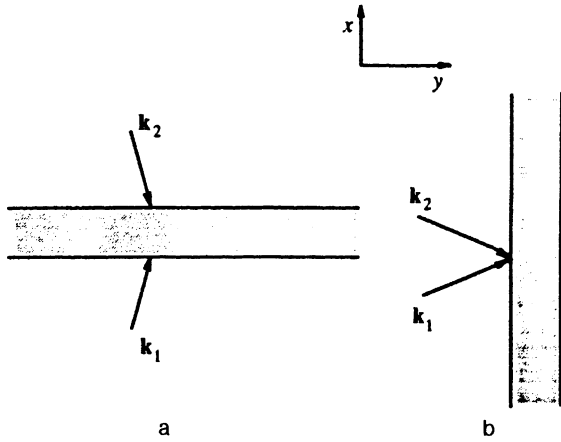
FIG. 1. Geometry of an experiment on high-harmonic generation in crossing beams.

tive of the study is to develop a simple algorithm for describing high-harmonic generation in interfering waves and to show that it can be more efficient than generation in a single traveling wave. Consequently, we shall not analyze in detail the problem of satisfying the mode-locking conditions in processes (1.2) in the general case. We merely note that if the angle at which the beams cross is not restricted in any way, the mode-locking conditions can be satisfied (by the proper choice of angles) in media whose dispersion varies over a very wide range. The angles of greatest practical interest are those in the vicinity of zero or π (Fig. 1). At small angles the mode-locking conditions can be satisfied in slightly dispersive media. Conversely, if the beams are directed almost head-on, these conditions are satisfied only in a highly dispersive medium. For example, in a plasma for $j=1$ they are satisfied if the electron density is equal to $4/(n+2)$ times the critical density at the fundamental (see below).

In formal analysis for the case of a homogeneous medium we do not restrict the angles at which the beams cross. In the case of an inhomogeneous medium we assume that the beams are incident on a plane layer from opposite sides symmetrically with respect to reflection in the layer (Fig. 1a) or from the same side symmetrically about the normal to the layer (Fig. 1b). The estimates apply to a plasma in which the beams are directed almost head-on.

2. STRUCTURE OF POLARIZATION WAVES: PHENOMENOLOGICAL ANALYSIS

Processes of the type (1.2) can be described as follows in the language of wave theory. Let two plane waves of amplitude a and b, polarized in the z direction, propagate in a medium. The y axis is directed along the bisector of the angle formed by the wave vectors. The following equation can then be written for the total electric field:

$$a\cos(\omega t - k_y y - k_x x) + b\cos(\omega t - k_y y + k_x x)$$
$$= E\cos(\omega t - k_y y - \varphi),\qquad (2.1)$$

where

$$E = \sqrt{a^2 + b^2 + 2ab\,\cos(2k_x x)},$$

$$\varphi = \arg[(a+b)\cos(k_x x) + i(a-b)\sin(k_x x)].$$

In this situation the polarization of the medium at the harmonic frequency $n\omega$ is represented by the expression

$$Nd_n(E)\exp[-in(\omega t - k_y y - \varphi)]$$

$$= N\exp[-in(\omega t - k_y y)]\sum_m d_{n,m}\exp(imk_x x),\qquad (2.2)$$

where N is the density of generating particles, d_n is the amplitude of the dipole moment, and

$$d_{n,m} = \frac{1}{2\pi}\int_0^{2\pi/k_x} d_n[E(x)]\exp[in\varphi(x)]$$

$$\times \exp(-imk_x x)k_x dx.\qquad (2.3)$$

The amplitudes $d_{n,m}$ depend only on the amplitudes a and b have nonzero values only for even values of $|n-m|$. Consequently, a set of polarization waves at the frequency $n\omega$ is excited in the medium. If for a certain m

$$\sqrt{n^2 k_y^2 + m^2 k_x^2} \simeq |k(n\omega)|\qquad (2.4)$$

and the amplitude $d_{n,m}$ is not small, radiation of frequency $n\omega$ can be efficiently generated in the direction (mk_x, nk_y). Generally speaking, this direction does not coincide with the direction of any of the excited waves. If the boundary of the layer in which generation takes place is arbitrarily oriented, the differences in the directions of propagation are preserved outside the layer as well and, in principle, can be used to isolate the required harmonic. We note that Eq. (2.4) can be satisfied only for $m \neq n$ in a medium whose refractive index varies monotonically with the frequency. The amplitudes $d_{n,m}$ will be calculated in the next section. Here we discuss the influence of inhomogeneity of the medium on the generation process.

We shall assume below that generation takes place in a plane layer with a density that varies along the x axis (Fig. 1a). The harmonics then propagate outside the layer in the same directions as the exciting waves. For the inhomogeneity of the medium to be taken into account, the product $k_x x$ must be replaced by the integral $\int^x k_x dx'$ in all the relations (2.1–2.3).

We disregard the dependence of the amplitudes a and b on x, assuming that the thickness of the layer and the deviation of the refractive index from unity are small. We write the field of the nth harmonic in the form

$$E_n\exp[-in(\omega t - k_y y)]\exp\left(i\int^x \sqrt{k^2(n\omega) - n^2 k_y^2}\,dx'\right).$$

Transforming from the wave equation for the field to the truncated equation for the amplitude E_n and integrating it with allowance for (2.2), we obtain

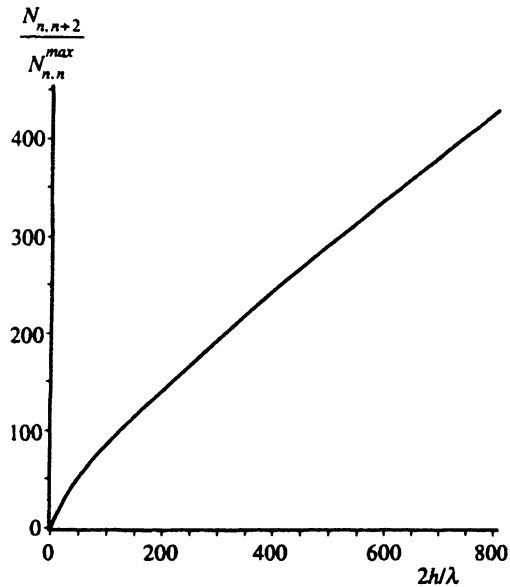$$E_n = \sum E_{n,m},\qquad (2.5)$$

where

FIG. 2. Ratio $N_{n,n+2}/N_{n,n}^{\max}$ vs thickness of an inhomogeneous layer.

$$E_{n,m} = i\frac{2\pi n^2\omega^2}{c^2\sqrt{k^2(n\omega)-n^2k_y^2}}d_{n,m}N_{nm},\tag{2.6}$$

$$N_{n,m} = \int N(x)\exp\left[i\int^x \kappa_{n,m}(x')dx'\right]dx,$$

$$\kappa_{n,m} = mk_x - \sqrt{k^2(n\omega)-n^2k_y^2}.\tag{2.7}$$

Consequently, the generation efficiency is determined by the value of the integral (2.7). Let us compare its possible values for $n = n$ and $m \neq n$. For definiteness we assume that the medium in question is a plasma with dielectric constant $\varepsilon(n\omega) = 1 - N_e/n^2N_{cr}$, where N_e and N_{cr} are the electron density and its critical value at the fundamental. We also assume that $N/N_e = $ const and $N_e/N_{cr} \ll k_x^2/(k_x^2+k_y^2)$. Then

$$\kappa_{n,m} = \frac{\omega}{c}(m-n)\left(1 - \frac{m}{2(m-n)}\frac{1}{\cos^2\theta}\frac{N_e}{N_{cr}}\right)\cos\theta,\tag{2.8}$$

where $\theta = \arctan(k_y/k_x)$ is the angle of incidence.

Simple calculations show that irrespective of the form of the function $N_e(x)$, the quantity $N_{n,n}$ does not exceed the value

$$N_{n,n}^{\max} = -\frac{2\lambda}{n\pi}N_{cr}\frac{N}{N_e}\cos\theta,\tag{2.9}$$

where λ is the wavelength of the fundamental radiation.

We have calculated $N_{n,m}$ numerically for $m \neq n$ in a plasma with a Gaussian density profile $N_e(x) = N_e(0)\exp(-x^2/h^2)$, where h is a constant. We set the quantity $[m/2(m-n)][N_e(0)/N_{cr}]\cos^{-2}\theta$ in (2.8) equal to $1+\beta$, where β is a small positive quantity, which can serve as an optimization parameter. The dependence of $N_{n,n+2}/N_{n,n}^{\max}$ on $2h/\lambda$, calculated for $\beta = 0.0023$, is shown in Fig. 2.

The calculations show that the inhomogeneity of the medium slows the growth of the possible values of N_{n,n_2} as the

interaction length increases. Nonetheless, for a moderate interaction length $2h \approx 800\lambda$ and $N_e(0) \approx 4N_{cr}\cos^2\theta/(n+2)$ we find that $N_{n,n+2}$ is approximately 400 times the value of $N_{n,n}^{\max}$.

We conclude with the observation that if waves are incident on a plane layer from one side at angles of incidence differing only in sign (Fig. 1b), according to the above-stated choice of coordinate axes, the density of the layer varies along the y axis in such a way that $k_x = $ const and $k_y = \sqrt{k^2-k_x^2}$. To analyze high-harmonic generation in this case, it is necessary to replace the product $k_y y$ in expressions (2.1) and (2.2) by the integral $\int^y k_y dy'$ and to write the field of the nth harmonic in the form of the sum

$$\sum_m E_{n,m}(y)\exp(-in\omega t)\exp(imk_x x)$$

$$\times\exp\left(i\int^y\sqrt{k^2(n\omega)-m^2k_x^2}dy'\right).\tag{2.10}$$

Expressions for $E_{n,m}$ can be obtained from (2.6) by replacing nk_y with mk_x; in (2.7) the integration with respect to x must be replaced by integration with respect to y, with $\kappa_{n,m}(y)$ given by the expression

$$\kappa_{n,m} = nk_y - \sqrt{k^2(n\omega)-m^2k_x^2}.$$

We call attention to the fact that waves of different orders m exit from the layer in different directions in this case $(mk_x, \sqrt{n^2\omega^2/c^2 - m^2k_x^2})$.

3. CALCULATION OF THE DIPOLE MOMENT AMPLITUDES

The integrals (2.3) can be evaluated if a not too complex and more or less realistic algorithm is available for computing the dependence $d_n(E)$. A great many theoretical papers have been written on high-harmonic generation. Unfortunately, they are based either on very elaborate numerical calculations, the results of which cannot be used here, or on relatively crude models that yield analytic results. The most realistic of the models amenable to analytic treatment is the one used in Ref. 8. The expressions derived there for the functions $d_n(E)$ are very elaborate and involve integration and summation between infinite limits. For our calculations of $d_n(E)$ we use a model that is conceptually similar that in Ref. 8, but is based on a different representation and can lead to simpler expressions that do not involve summation.

In the ensuing analysis we use the model of a single-electron atom, whose states satisfy the Schrödinger equation

$$i\hbar\dot\Psi = \left(\frac{\hat p^2}{2m}+\hat V+\hat H_F\right)\Psi,\tag{3.1}$$

where $\hat H_F$ is the interaction energy of an electron with the wave field. We replace this equation by the equivalent system

$$\Psi = \Psi_V + \Psi_F,\tag{3.2}$$

$$i\hbar\dot\Psi_V = \left(\frac{\hat p^2}{2m}+\hat V\right)\Psi_V + \hat V\Psi_F,\tag{3.3}$$

$$i\hbar\dot{\Psi}_F = \left(\frac{\hat{p}^2}{2m} + \hat{H}_F\right)\Psi_F + \hat{H}_F\Psi_V \tag{3.4}$$

(the sum of Eqs. (3.3) and (3.4) coincides with (3.1)).

The interaction Hamiltonian can be written in the A representation in the long-wavelength approximation:

$$H_F = \frac{e}{mc}\mathbf{A}\cdot\hat{\mathbf{p}}. \tag{3.5}$$

The term proportional to A^2 is omitted. This limits the validity of the model (we shall not overstep these bounds below), but simplifies the ensuing analysis considerably.

We assume that $\Psi_F = 0$ up until the time the field is applied, whereupon it follows from Eqs. (3.4) and (3.5) that

$$|\Psi_F\rangle = \frac{1}{i\hbar}\int_{-\infty}^{t}dt'\,d^3p\,\exp\left[-\frac{i}{\hbar}\frac{p^2}{2m}(t-t')\right.$$
$$\left.-\frac{i}{\hbar}\frac{ep}{mc}\int_{t'}^{t}A\,d\tau\right]|\varphi_p\rangle\left\langle\varphi_p\left|\frac{e\hat{p}}{mc}A(t')\right|\Psi_V(t')\right\rangle, \tag{3.6}$$

where φ_p is a momentum eigenfunction. The function Ψ_F can be written in the form

$$\Psi_V = a_0\exp\left(\frac{iE_0 t}{\hbar}\right)\varphi_0 + \delta\psi, \tag{3.7}$$

where φ_0 and E_0 are the eigenstate and energy of the atom, and $\langle\varphi_0|\delta\psi\rangle = 0$. Within the scope of the present study we disregard the term $\delta\psi$ in (3.7) and assume that the amplitude a_0 varies slowly, i.e., $|\dot{a}_0/a_0| \ll \omega$. The validity of this assumption in the specific situation is tested by means of the equation

$$\dot{a}_0 = \frac{1}{i\hbar}\exp\left(i\frac{E_0}{\hbar}t\right)\langle\varphi_0|V|\Psi_F\rangle, \tag{3.8}$$

which is a consequence of (3.3). Finally, in computing the integrals, we assume that

$$\int_{t'}^{t}A\,d\tau = -\frac{cE}{\omega^2}(\cos\omega t - \cos\omega t'). \tag{3.9}$$

The following expression for the average momentum can now be obtained from Eqs. (3.2), (3.6), and (3.7) for $\delta\psi = 0$ and $a_0 = \text{const}$:

$$\langle\Psi|\hat{p}_z|\Psi\rangle = |a_0|^2\sum p_n e^{-in\omega t}, \tag{3.10}$$

where

$$p_n = \frac{1}{\hbar\omega}\int_0^{\infty}d\tau\exp\left(in\omega\frac{\tau}{2}\right)\int d^3p\,p_z\left(\frac{p_0^2+p^2}{2\hbar m}\right)^2\langle\varphi_0|\varphi_p\rangle$$
$$\times\langle\varphi_p|\varphi_0\rangle\left[\exp\left(-\frac{i}{\hbar}\frac{p_0^2+p^2}{2m}\tau\right)+\text{c.c}\right]$$
$$\times J_n\left(\frac{2eEp}{\hbar m\omega^2}\sin\frac{\omega\tau}{2}\right), \tag{3.11}$$

J_n is a Bessel function, and $p_0^2 = 2m|E_0|$. In the derivation of Eqs. (3.10) and (3.11) we have not assumed that the term Ψ_F in (3.2) is small, nor have we resorted to approximate methods for evaluating the integrals. Consequently, the spectrum p_n represented in (3.11) is determined entirely by the stated assumptions and not by the approximate computational procedure. (This consideration is important, because the amplitudes of high harmonics are relatively small, so that the approximate transformation of the function $p_z(t)$, while not altering it appreciably, can significantly distort the spectrum of these harmonics.) The subsequent simplifications in (3.11) no longer require high accuracy. We implement them on the assumption that φ_0 is the ground state of the hydrogen atom, so that $|\langle\varphi_0|\varphi_p\rangle|^2 = 8\pi^{-2}p_0^5(p^2+p_0^2)^{-4}$.

The integration over the transverse components of the momentum in (3.11) is carried out by the stationary phase method. To integrate with respect to the longitudinal component p_z, we assume that the quantity $(p_0^2+p^2)^{-2}$ in the integrand can be regarded as a slow variable. The integral then reduces to a tabulated form. We ultimately obtain

$$p_n \simeq -\frac{eE}{n\omega}\sqrt{\frac{64I}{\pi\hbar\omega}}\int_0^{\infty}dx\frac{1}{x^{5/2}}$$
$$\times\frac{\sin(x/2)}{\left(1+\dfrac{2U}{I}\dfrac{1-\cos x}{x^2}\right)^2}e^{inx/2}F_n(x), \tag{3.12}$$

where

$$F_n(x) = \exp\left(-i\frac{n}{4}\pi - i\frac{I}{\hbar\omega}x + iY\right)[J_{(n+1)/2}(Y)$$
$$-iJ_{(n-1)/2}(Y)] - \text{c.c},$$

$$Y = \frac{2U}{\hbar\omega}\frac{1-\cos x}{x}, \quad U = \frac{e^2E^2}{4m\omega^2}.$$

The denominator of the integrand in (3.12) is written on the assumption that the main contribution to the integral with respect to p_z is from the vicinity of $p_{\max}$, where

$$p_{\max} = \frac{eE}{\omega}\frac{2\sin(x/2)}{x}.$$

This assumption can be justified for $n \leq 2U/\hbar\omega$. For all other harmonics it can be shown that

$$p_{\max} \leq \frac{eE}{\omega}\frac{2\sin(x/2)}{x}.$$

The vector potential in (3.5) is monochromatic by assumption, so that the amplitudes of the mechanical and canonical momenta coincide at harmonic frequencies. The amplitudes of the dipole moment are therefore related to (3.12) by the linear equation

$$d_n = -i\frac{e}{m}\frac{p_n}{n\omega}. \tag{3.13}$$

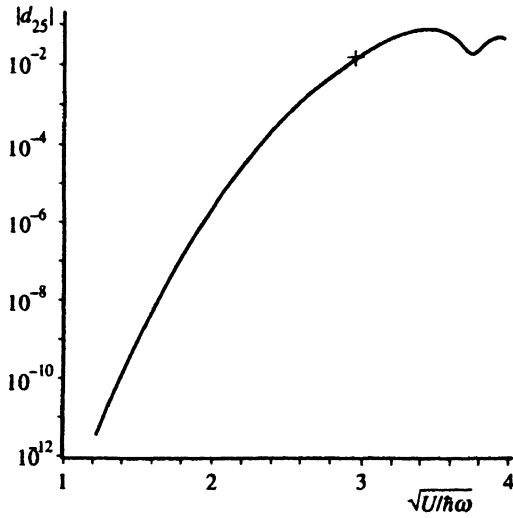The remainder of the discussion applies to the 25th harmonic. A graph of $d_{25}(E)$ calculated numerically from Eqs.

FIG. 3. Amplitude of the 25th harmonic of the dipole moment (in units of $p_0 e/m_e \omega$) vs amplitude of the electric field.

FIG. 4. Amplitudes $d_{25,m}(a,b)$ normalized to $d_{25}(\sqrt{a^2+b^2})$. a) $b/a=1$; b) 0.1; c) 0.04.

(3.12) and (3.13) for $I=20\hbar\omega$ is shown in Fig. 3. It agrees qualitatively with the results of other papers, for example, Refs. 8 and 10.

It is important to note that the assumption of slow variation of the amplitude a_0 fails to the right of the first maximum of the $d_{25}(E)$ curve. We mainly use the parts of the graph to the left of the first maximum to calculate $d_{25,m}(a,b)$ from Eq. (2.3).

Figure 4 shows the spectra of the amplitudes $d_{25,m}(a,b)$, normalized to $d_{25}(\sqrt{a^2+b^2})$ and calculated using Eqs. (2.3), (3.12), and (3.13) for various ratios b/a and a fixed value of a^2+b^2. The operating point $(\sqrt{a^2+b^2},\, d_{25}(\sqrt{a^2+b^2}))$ is marked by a cross on the $d_{25}(E)$ curve in Fig. 3. Naturally, the results depend on the choice of this point, but the qualitative trends illustrated in Fig. 4 are typical. For $b=a$ the amplitudes with m close to n are small. The dependence of $d_{n,m}$ on m exhibits complex behavior at small m. Its shape is strongly related to the large range of the amplitude E, which attains values at which $d_n(E)$ does not vary monotonically, and Eq. (3.12) is incorrect. By and large, therefore, Fig. 4a is illustrative in nature.

As b decreases, the maximum in the distribution of $d_{n,m}$ shifts toward values of m close to n and gradually narrows. At $b=0$ only the amplitude with $m=n$ still has a nonzero value. It is evident from Fig. 4b that for small ratios b/a the amplitudes $d_{n,m}$ with $m=n-2,\, n+2$ can attain values comparable with $d_n(\sqrt{a^2+b^2})$.

IV. DISCUSSION OF THE RESULTS AND CONCLUSIONS

For parameters of the medium corresponding to the rightmost point in Fig. 2 and for parameters of the field corresponding to Fig. 4c the amplitude $E_{25,27}$ is more than two orders of magnitude higher than the maximum possible amplitude of the 25th harmonic generated for the given value of N/N_e in a single beam of intensity corresponding to the operating point represented by the cross in Fig. 3. As the interaction length increases, of course, further growth of the amplitude $E_{25,27}$ is observed. In principle, this length is bounded
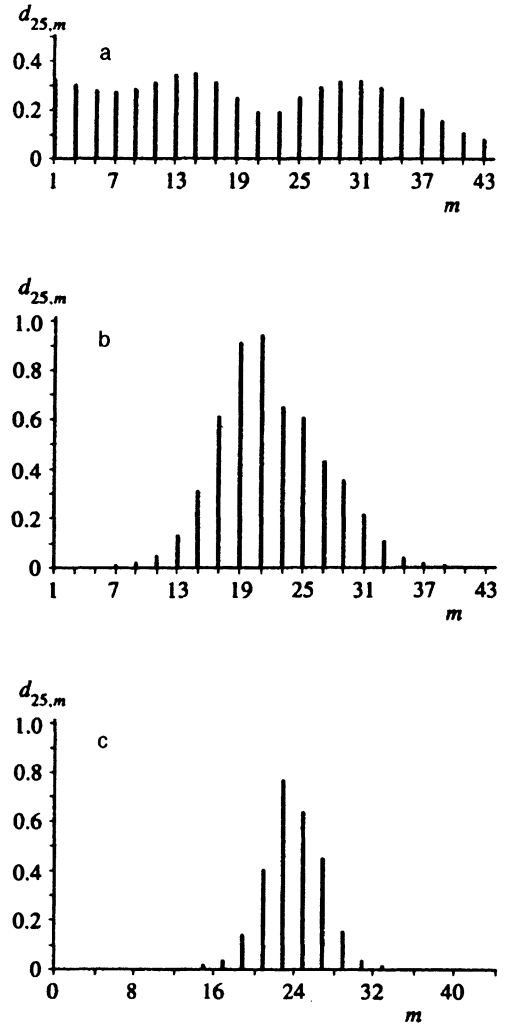
by the durations of the pulses $a^2(t)$ and $b^2(t)$. If the pulses propagate almost head-on, the length at which, for example, the leading edge of the pulse $a^2(t)$ is situated in the field of the pulse $b^2(t)$ is approximately equal to $c\tau_b/2$, where τ_b is the duration of the pulse $b^2(t)$. In this sense it is important to realize that the maximum values of the amplitudes $d_{n,n+2}$ are attained for small ratios $b^2/a^2 \simeq 10^{-3}$, so that in experimental work one can use relatively low-intensity pulses $b^2(t)$ with a duration much longer than that of the stronger pulse $a^2(t)$ and sufficient for providing a long interaction length. The cross section of the low-intensity beam can also be made fairly large (and not necessarily circular) to ensure not using overly small angles at which the beams collide. In principle, it is even possible to use pulses with different carrier frequencies, but this complicates the theoretical analysis of the problem. (Perry and Crane[11] have described experiments on the generation of high harmonics and combination frequencies in a two-color beam made up of light with wavelengths of 0.527 μm and 1.053 μm.)

Interference of the incident and reflected waves can also be assumed to play an important role in high-harmonic generation in a plasma produced when the surface of a thick

target is irradiated with high-intensity laser pulses.[12,13] According to the model developed in Ref. 14, such generation is associated with collective motions in the plasma. However, this model is not the only one possible. In every case experiments[12] have definitely revealed the formation of an extended corona, in which it is possible for high harmonics to be generated by the same mechanisms as in a rarefied gas jet (the generation of even harmonics is attributable to the presence of a static field[15]). In Ref. 13 the corona could have been generated, in principle, by the "pedestal" of the laser pulse.

A plasma layer with the parameters used in the calculations can be created, for example, by in vacuo laser heating of a film or foil. An almost-Gaussian density distribution is formed in such processes.[16]

We have thus developed a theoretical model suitable for describing high-harmonic generation in a field of two waves interfering in a homogeneous or inhomogeneous dispersive medium (gas or plasma layer), and we have shown that two crossing or head-on beams can be utilized in high-harmonic generation experiments to cancel or partially compensate the dispersion of the working medium, to significantly enhance the generation efficiency, and to produce harmonics that emanate from the layer at different angle.

[1] A. McPherson, G. Gibson, H. Jara *et al.*, J. Opt. Soc. Am. B **4**, 595 (1987).
[2] M. Ferray, A. L. Huiller, X. F. Li *et al.*, J. Phys. B **21**, L31 (1988).
[3] A. L. Huiller and P. Balcou, Phys. Rev. Lett. **70**, 774 (1993).
[4] J. Zhou, J. Peatross, M. M. Murnane *et al.*, Phys. Rev. Lett. **76**, 752 (1996).
[5] A. M. Zheltikov, N. I. Koroteev, and A. B. Fedotov, Proc. SPIE **2097**, 308 (1993); Laser Phys. **4**, 564 (1994).
[6] S. Kubodera, Y. Nagat, Y. Akiyama *et al.*, Phys. Rev. A **48**, 4576 (1993); Y. Akiyama, K. Midorikawa, Y. Matsunaya *et al.*, Phys. Rev. Lett. **69**, 2176 (1992).
[7] J. L. Krause, K. J. Shapher, and K. C. Kulander, Phys. Rev. Lett. **68**, 3535 (1992).
[8] M. Lewenstein, P. Balcou, M. Ivanov *et al.*, Phys. Rev. A **49**, 2117 (1994).
[9] J. F. Reintjes, *Nonlinear Optical Parametric Processes in Liquids and Gases*, Academic Press, New York (1984).
[10] R. Burlon, G. Ferrante, C. Leone *et al.*, J. Opt. Soc. Am. B **13**, 162 (1996).
[11] M. D. Perry and J. K. Crane, Phys. Rev. A **48**, R4051 (1993).
[12] R. L. Carman, C. K. Rhodes, and R. F. Benjamin, Phys. Rev. A **24**, 2469 (1981).
[13] D. Von der Linde, G. Jenke, T. Enger, and P. Agostini, in *Technical Digest of the Ninth International Symposium on Ultrafast Processes in Spectroscopy*, International Center for Theoretical Physics, Trieste, Italy (1995), W A2.
[14] B. Bezzerides, R. D. Jones, and D. W. Forslund, Phys. Rev. Lett. **43**, 202 (1982).
[15] R. Burlon, G. Ferrante, C. Leone, and V. T. Platonenko, in *Technical Digest of the International Conference on LASERS 95*, Society for Optical and Quantum Electronics, Charleston, N.C. (1995).
[16] W. Fader, Phys. Fluids **11**, 2200 (1968).

Translated by James S. Wood